

Kinetics and Mechanism of the Oxidation of Ascorbic Acid in Aqueous Solutions by a *trans*-Dioxoruthenium(VI) Complex

Yi-Ning Wang, Kai-Chung Lau, William W. Y. Lam, Wai-Lun Man, Chi-Fai Leung, and Tai-Chu Lau\*

Department of Biology and Chemistry, City University of Hong Kong, Tat Chee Avenue, Kowloon, Hong Kong, P. R. China

Received August 21, 2008

The oxidation of ascorbic acid ( $H_2A$ ) by a *trans*-dioxoruthenium(VI) species,  $trans-[Ru^{VI}(tmc)(O)_2]^{2+}$  ( $tmc = 1,4,8,11$ -tetramethyl-1,4,8,11-tetraazacyclotetradecane), has been studied in aqueous solutions under argon. The reaction occurs in two phases:  $trans-[Ru^{VI}(tmc)(O)_2]^{2+} + H_2A \rightarrow trans-[Ru^{IV}(tmc)(O)(OH_2)]^{2+} + A$ ,  $trans-[Ru^{IV}(tmc)(O)(OH_2)]^{2+} + H_2A \rightarrow trans-[Ru^{II}(tmc)(OH_2)_2]^{2+} + A$ . Further reaction involving anation by  $H_2A$  occurs, and the species  $[Ru^{III}(tmc)(A^{2-})(MeOH)]^+$  can be isolated upon aerial oxidation of the solution at the end of phase two. The rate laws for both phases are first-order in both  $Ru^{VI}$  and  $H_2A$ , with the second-order rate constants  $k_2 = (2.58 \pm 0.04) \times 10^3 M^{-1} s^{-1}$  at  $pH = 1.19$  and  $k_2' = (1.90 \pm 0.03) M^{-1} s^{-1}$  at  $pH = 1.24$ ,  $T = 298 K$  and  $I = 0.1 M$  for the first and second phase, respectively. Studies on the effects of acidity on  $k_2$  and  $k_2'$  suggest that  $HA^-$  is the kinetically active species. Kinetic studies have also been carried out in  $D_2O$ , and the deuterium isotope effects for oxidation of  $HA^-$  by  $Ru^{VI}$  and  $Ru^{IV}$  are  $5.0 \pm 0.3$  and  $19.3 \pm 2.9$ , respectively, consistent with a hydrogen atom transfer (HAT) mechanism for both phases. A linear correlation between  $\log(\text{rate constants})$  for oxidation by  $Ru^{VI}$  and the O–H bond dissociation energies of  $HA^-$  and hydroquinones is obtained, which also supports a HAT mechanism.

## Introduction

Ascorbic acid (vitamin C) is an important, water-soluble antioxidant in chemical and biological systems.<sup>1</sup> It functions as a free radical scavenger in biological systems mainly by hydrogen atom transfer (or proton-coupled electron transfer).<sup>2</sup> On the other hand, the oxidation of ascorbic acid ( $H_2A$ ) by a variety of transition metal complexes in aqueous solutions appears to occur by an

electron transfer mechanism. In most cases, the predominant reactive species is the ascorbate ion  $HA^-$ , which is oxidized by electron transfer followed by deprotonation to give the ascorbyl radical ( $A^{\cdot-}$ ), which is then rapidly converted to dehydroascorbic acid (A). Oxidation by complexes of iron(III),<sup>3–8</sup> iridium(IV) and molybdenum(V),<sup>9</sup> nickel(IV),<sup>10,11</sup> platinum(IV),<sup>12,13</sup> cobalt(III),<sup>14,15</sup> and ruthenium(III)<sup>16–18</sup> has been proposed to occur by outer-sphere electron transfer. Inner-sphere electron trans-

\* To whom correspondence should be addressed. E-mail: bhtclau@cityu.edu.hk.

- (1) Davies, M. B.; Austin, J.; Partridge, D. A. *Vitamin C: Its Chemistry and Biochemistry*; Royal Society of Chemistry: Cambridge, 1991; pp 3–15.
- (2) (a) Njus, D.; Jalukar, V.; Zu, J.; Kelley, P. M. *Am. J. Clin. Nutr.* **1991**, *54*, 1179–1183. (b) Njus, D.; Kelley, P. M. *FEBS Lett.* **1991**, *284*, 147–151.
- (3) Pelizzetti, E.; Mentasti, E.; Pramauro, E. *Inorg. Chem.* **1976**, *15*, 2898–2900.
- (4) Kimura, M.; Yamamoto, M.; Yamabe, S. *J. Chem. Soc., Dalton Trans.* **1982**, 423–427.
- (5) Martins, L. J. A.; Barbosa da Costa, J. *J. Chem. Educ.* **1988**, *65*, 176–178.
- (6) Lin, L.-M.; Lien, M.-H.; Yeh, A. *Int. J. Chem. Kinet.* **2005**, *37*, 126–133.
- (7) Bhattacharyya, J.; Das, S.; Mukhopadhyay, S. *Dalton Trans.* **2007**, 1214–1220.
- (8) Creutz, C. *Inorg. Chem.* **1981**, *20*, 4449–4452.

- (9) Pelizzetti, E.; Mentasti, E.; Pramauro, E. *Inorg. Chem.* **1978**, *17*, 1181–1186.
- (10) Acharya, S.; Neogi, G.; Panda, R. K. *J. Chem. Soc., Dalton Trans.* **1984**, 1471–1476.
- (11) Macartney, D. H.; Sutin, N. *Inorg. Chim. Acta* **1983**, *74*, 221–228.
- (12) Lemma, K.; House, D. A.; Retta, N.; Elding, L. I. *Inorg. Chim. Acta* **2002**, *331*, 98–108.
- (13) Lemma, K.; Sargeson, A. M.; Elding, L. I. *J. Chem. Soc., Dalton Trans.* **2000**, *116*, 7–1172.
- (14) Martinez, P.; Zuluaga, J.; Noheda, P. *Inorg. Chim. Acta* **1992**, *195*, 249–253.
- (15) Martinez, P.; Zuluaga, J.; Kraft, J.; Van Eldik, R. *Inorg. Chim. Acta* **1988**, *146*, 9–12.
- (16) Akhtar, M. J.; Haim, A. *Inorg. Chem.* **1988**, *27*, 1608–1610.
- (17) Chatterjee, D. *J. Chem. Soc., Dalton Trans.* **1996**, 4389–4392.
- (18) Chatterjee, D.; Sengupta, A.; Mitra, A.; Basak, S. *Inorg. Chem. Commun.* **2006**, *9*, 1219–1222.

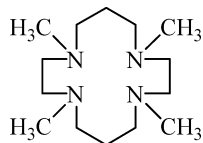


Figure 1. Structure of tmc.

fer has also been proposed for a number of substitution-labile oxidants.<sup>19–24</sup> Recently, the oxidation of 5,6-isopropylidene ascorbate by  $[\text{Fe}^{\text{III}}(\text{TPP})(\text{Im})(\text{ImH})]$  (TPP = tetraphenylporphyrin, ImH = 4-methylimidazole) in acetonitrile is shown to occur by a hydrogen atom transfer (HAT) mechanism.<sup>25</sup>

Despite the numerous reports mentioned above, there are few studies on the oxidation of ascorbic acid by metal–oxo species. This is somewhat surprising since metal–oxo species are important oxidants in chemical and biological systems.<sup>26,27</sup> The oxidation of ascorbic acid by a  $(\text{EDTA})\text{Ru}^{\text{V}}=\text{O}$  species has been reported, and a mechanism involving rate-determining outer-sphere electron transfer was proposed.<sup>28</sup> We report here a study of the oxidation of L-ascorbic acid in aqueous solutions by a cationic *trans*-dioxoruthenium(VI) complex, *trans*- $[\text{Ru}^{\text{VI}}(\text{tmc})(\text{O})_2]^{2+}$  (tmc = 1,4,8,11-tetramethyl-1,4,8,11-tetraazacyclotetradecane, Figure 1). We provide evidence that this reaction occurs in two phases,  $\text{Ru}^{\text{VI}} \rightarrow \text{Ru}^{\text{IV}}$  and  $\text{Ru}^{\text{IV}} \rightarrow \text{Ru}^{\text{II}}$ ; the mechanism for both phases involves rate-limiting H-atom transfer from ascorbate to  $\text{Ru}=\text{O}$ . The oxidation of various organic and inorganic substrates by *trans*- $[\text{Ru}^{\text{VI}}(\text{tmc})(\text{O})_2]^{2+}$  has been reported.<sup>29–34</sup> Thermodynamic data ( $E^\circ$  vs NHE and  $\text{p}K_{\text{a}}$  values, 298 K) for the *trans*- $[\text{Ru}^{\text{VI}}(\text{tmc})(\text{O})_2]^{2+}$  system are summarized in Scheme 1.<sup>35,36</sup>

## Experimental Section

**Materials.** *trans*- $[\text{Ru}^{\text{VI}}(\text{tmc})(\text{O})_2](\text{PF}_6)_2$  and *trans*- $[\text{Ru}^{\text{IV}}(\text{tmc})(\text{O})(\text{NCCH}_3)](\text{PF}_6)_2$  were prepared by literature methods.<sup>37</sup> Solutions of *trans*- $[\text{Ru}^{\text{IV}}(\text{tmc})(\text{O})(\text{OH}_2)]^{2+}$  were prepared by dissolving *trans*- $[\text{Ru}^{\text{IV}}(\text{tmc})(\text{O})(\text{NCCH}_3)](\text{PF}_6)_2$  in water. L-Ascorbic acid (Aldrich), trifluoroacetic acid (Aldrich), sodium acetate (Aldrich), and acetic acid (RDH) were used as received. Water for kinetic experiments was distilled twice from alkaline permanganate and was deaerated with argon for 30 min before use. Ionic strength was maintained with sodium trifluoroacetate.  $\text{D}_2\text{O}$  (99.9 atom % D) was obtained from Aldrich. The  $\text{pD}$  values for  $\text{D}_2\text{O}$  solutions were obtained from a pH meter (Delta 320) using the relationship  $\text{pD} = \text{pH}_{\text{meas}} + 0.4$ .

**Instrumentation.** The kinetics of the reaction were studied by using either a Hewlett-Packard 8452A diode-array spectrophotometer, a Perkin-Elmer Lambda 19 UV–vis–NIR spectrometer, a Hi-Tech Scientific SF-61 stopped-flow spectrophotometer, or an Applied Photophysics SX20 stopped-flow spectrophotometer. Electrospray ionization mass spectra (ESI/MS) were obtained from a PE SCIEX API 365 mass spectrometer. The analyte solution was continuously infused with a syringe pump at a constant flow rate of  $9 \mu\text{L min}^{-1}$  into the pneumatically assisted electrospray probe with nitrogen as the nebulizing gas. The declustering potential was typically set at 10–20 V.  $^1\text{H}$  NMR spectra were obtained from a Varian (300 MHz) FT-NMR spectrometer.

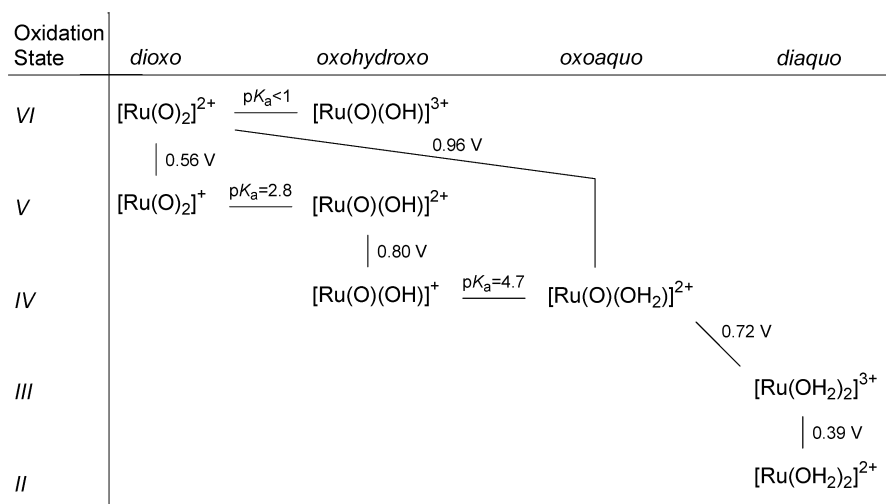
**Kinetics.** The concentrations of  $\text{H}_2\text{A}$  were at least in 10-fold excess of  $\text{Ru}^{\text{VI}}$ . The reaction progress was monitored by observing absorbance changes at 388 nm for the first phase ( $\lambda_{\text{max}}$  of  $\text{Ru}^{\text{VI}}$ ), 290 or 340 nm for the second phase (both wavelengths gave identical results and most runs were monitored at 340 nm). Pseudo-first-order rate constants,  $k_{\text{obs}}$ , were obtained by nonlinear least-squares fits of  $A_t$  versus time  $t$  according to the equation  $A_t = A_\infty + (A_0 - A_\infty)\exp(-k_{\text{obs}}t)$ , where  $A_0$  and  $A_\infty$  are the initial and final absorbance, respectively.

**Product Analysis.** The ruthenium product for the first phase of the reaction was determined by the following procedure. A known amount of *trans*- $[\text{Ru}^{\text{VI}}(\text{tmc})(\text{O})_2]^{2+}$  ( $1.7 \times 10^{-3}$  mmol) was allowed to react with 1 mol equiv of  $\text{H}_2\text{A}$  in 0.01 M  $\text{CF}_3\text{CO}_2\text{H}$  at room temperature. The resulting solution was loaded onto a Sephadex-SP C-25 cation-exchange column. By eluting with 0.2 M  $\text{CF}_3\text{CO}_2\text{H}$  and then examining the UV–vis spectrum of the solution, *trans*- $[\text{Ru}^{\text{IV}}(\text{tmc})(\text{O})(\text{OH}_2)]^{2+}$  ( $\lambda_{\text{max}} = 290$  nm,  $\epsilon = 1600 \text{ M}^{-1} \text{ cm}^{-1}$ ) was found to be produced quantitatively.<sup>37</sup>

The product resulting from oxidation of  $\text{H}_2\text{A}$  was determined as follows: 290  $\mu\text{L}$  solution of  $\text{H}_2\text{A}$  ( $6.3 \times 10^{-3}$  mmol) in  $\text{D}_2\text{O}$  (99 atom% D) was added to 6 mL of *trans*- $[\text{Ru}^{\text{VI}}(\text{tmc})(\text{O})_2]^{2+}$  ( $2.1 \times 10^{-3}$  mmol) in  $\text{D}_2\text{O}$  (99 atom % D). The mixture was stirred for 3 h, and the volatiles were removed by reduced pressure. The residue was dissolved in 1 mL of  $\text{D}_2\text{O}$  (99.9 atom% D) containing acetonitrile ( $4.21 \times 10^{-2}$  M) as internal standard. The formation of dehydroascorbic acid was monitored by  $^1\text{H}$  NMR at 4.63, 4.48, and 4.03 ppm with reference to the acetonitrile standard (1.93 ppm).<sup>38–40</sup> The amount of dehydroascorbic acid produced was found to be  $(4.2 \pm 0.4) \times 10^3$

- (19) Xu, J.; Jordan, R. B. *Inorg. Chem.* **1990**, *29*, 4180–4184.  
 (20) Bansch, B.; Martinez, P.; Uribe, D.; Zuluaga, J.; Van Eldik, R. *Inorg. Chem.* **1991**, *30*, 4555–4559.  
 (21) Khan, M. M. T.; Shukla, R. S. *Inorg. Chim. Acta* **1988**, *149*, 89–94.  
 (22) Ghosh, S. K.; Gould, E. S. *Inorg. Chem.* **1989**, *28*, 1538–1542.  
 (23) Hynes, M. J.; Wurm, K.; Moloney, A. *Inorg. Chim. Acta* **1993**, *211*, 5–10.  
 (24) Gangopadhyay, S.; Saha, S. K.; Ali, M.; Banerjee, P. *Int. J. Chem. Kinet.* **2004**, *23*, 105–112.  
 (25) Warren, J. J.; Mayer, J. M. *J. Am. Chem. Soc.* **2008**, *130*, 2774–2776.  
 (26) *Organic Synthesis by Oxidation with Metal Compounds*; Mijs, W. J., de Jonge, C. R. H. I., Eds.; Plenum Press: New York, 1986.  
 (27) *Biomimetic Oxidations Catalyzed by Transition Metal Complexes*; Meunier, B., Ed.; Imperial College Press: London, 2000.  
 (28) Khan, M. M.; Chatterjee, D.; Shukla, R. S. *J. Mol. Catal.* **1991**, *69*, 33–39.  
 (29) Che, C. M.; Tang, W. T.; Lee, W. O.; Wong, K. Y.; Lau, T. C. *J. Chem. Soc., Dalton Trans.* **1992**, 1551–1556.  
 (30) Che, C. M.; Li, C. K.; Tang, W. T.; Yu, W. Y. *J. Chem. Soc., Dalton Trans.* **1992**, 3153–3158.  
 (31) Lau, T. C.; Lau, K. W. C.; Lo, C. K. *Inorg. Chim. Acta* **1993**, *209*, 89–92.  
 (32) Lau, T. C.; Chow, K. H.; Lau, K. W. C.; Tsang, W. Y. K. *J. Chem. Soc., Dalton Trans.* **1997**, 313–315.  
 (33) Lau, T. C.; Lau, K. W. C.; Lau, K. J. *J. Chem. Soc., Dalton Trans.* **1994**, 3091–3093.  
 (34) Lam, W. W. Y.; Lee, M. F. W.; Lau, T. C. *Inorg. Chem.* **2006**, *45*, 315–321.  
 (35) Che, C. M.; Wong, K. Y.; Poon, C. K. *Inorg. Chem.* **1985**, *24*, 1797–1800.  
 (36) Che, C. M.; Lau, K.; Lau, T. C.; Poon, C. K. *J. Am. Chem. Soc.* **1990**, *112*, 5176–5181.

- (37) Che, C. M.; Lai, T. F.; Wong, K. Y. *Inorg. Chem.* **1987**, *26*, 2289–2299.  
 (38) Kurata, T.; Nishikawa, Y. *Biosci. Biotechnol. Biochem.* **2000**, *64*, 1651–1655.  
 (39) Nishikawa, Y.; Kurata, T. *Biosci. Biotechnol. Biochem.* **2000**, *64*, 476–483.  
 (40) Litos, C.; Aletras, V.; Hatzipanayioti, D.; Kamariotaki, M.; Lymberopoulou-Karaliota, A. *Inorg. Chim. Acta* **2007**, *360*, 2321–2330.

**Scheme 1.** Thermodynamic Data for the  $trans\text{-}[\text{Ru}^{\text{VI}}(\text{tmc})(\text{O})_2]^{2+}$  System (Potentials vs NHE and at pH = 0)

mmol (after subtracting the amount of dehydroascorbic acid formed in a blank without the oxidant); i.e., 2 mol of dehydroascorbic acid is formed from each mole of  $\text{Ru}^{\text{VI}}$  oxidant.

**Synthesis of  $[\text{Ru}^{\text{III}}(\text{tmc})(\text{A}^{2-})(\text{MeOH})(\text{BPh}_4)]$ .** Solid  $\text{H}_2\text{A}$  (200 mg, 1.14 mmol) was added to a yellow suspension of  $[\text{Ru}^{\text{VI}}(\text{tmc})(\text{O})_2](\text{PF}_6)_2$  (80 mg, 0.12 mmol) in MeOH (5 mL), and the solution was stirred in air for 16 h. Slow addition of a methanolic solution (5 mL) of  $\text{NaBPh}_4$  (165 mg, 0.48 mmol) to the resulting green solution gave a pale green solid, which was filtered, washed with MeOH (3 × 5 mL), and then dried under vacuum. The same compound was obtained when the synthesis was carried out in water (and the product was washed with methanol). Yield: (67%). Anal. Calcd for  $\text{C}_{45}\text{H}_{62}\text{N}_4\text{O}_7\text{BRu}$ : C, 61.22; H, 7.08; N, 6.35. Found: C, 61.43; H, 6.96; N, 6.33. ESI-

MS:  $m/z = 532$  ( $\text{M}^+ - \text{MeOH}$ ).  $\mu_{\text{eff}} = 1.85 \mu_{\text{B}}$  (solid sample, Gouy method).

## Results

**Spectrophotometric Changes and Stoichiometry.** Rapid spectrophotometric changes occurred when an aqueous acidic solution of  $trans\text{-}[\text{Ru}^{\text{VI}}(\text{tmc})(\text{O})_2]^{2+}$  ( $\text{Ru}^{\text{VI}}$ ) was mixed with excess L-ascorbic acid ( $\text{H}_2\text{A}$ ) under argon. Repetitive scanning at different time scales indicated that the reaction occurred in two distinct phases, as shown in Figure 2. Well-defined isosbestic points were maintained at 415 nm for the first phase, and at 312, 390 nm for the second phase. When 1 equiv of  $\text{H}_2\text{A}$  was used, only the

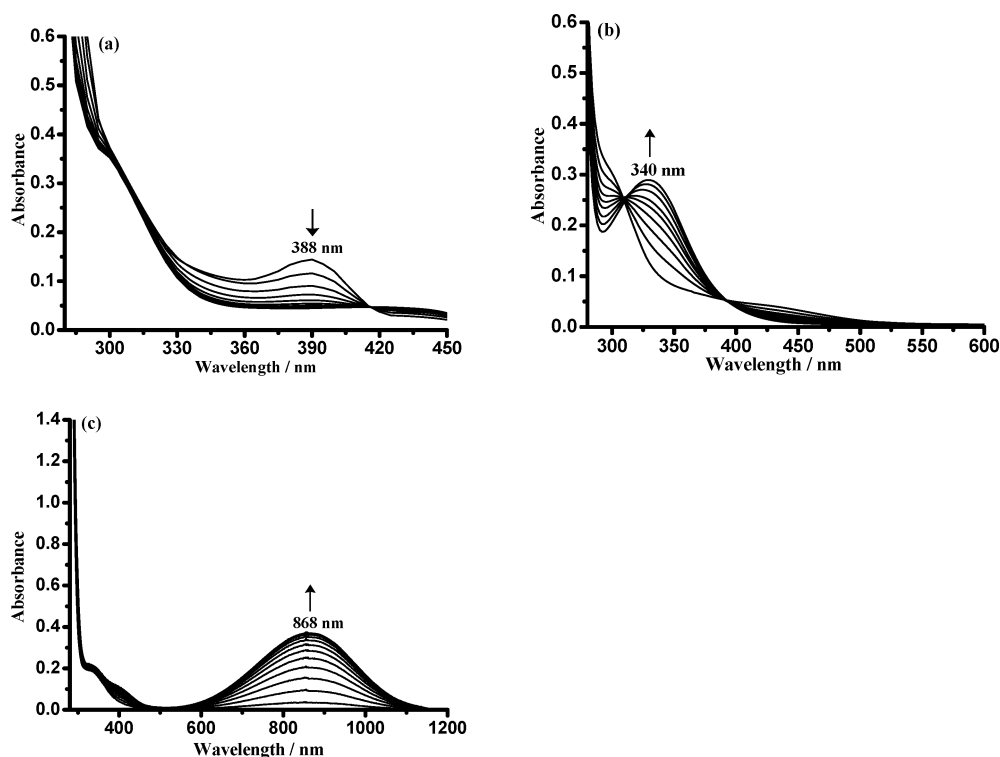


**Figure 2.** Spectrophotometric changes for the oxidation of  $\text{H}_2\text{A}$  by  $trans\text{-}[\text{Ru}^{\text{VI}}(\text{tmc})(\text{O})_2]^{2+}$  ( $[\text{Ru}^{\text{VI}}] = 2.89 \times 10^{-4}$  M,  $[\text{H}_2\text{A}] = 3.08 \times 10^{-3}$  M, pH = 1.25 at 298.0 K,  $I = 0.1$  M). (a) Spectra collected at 0.06 s intervals using a stopped-flow spectrophotometer. (b) Spectra collected at 60 s intervals using a diode-array spectrophotometer. (c) Spectra collected at 1000 s intervals upon exposure to air after  $\text{Ru}^{\text{VI}}$  had reacted with  $\text{H}_2\text{A}$  for 800 s under argon.

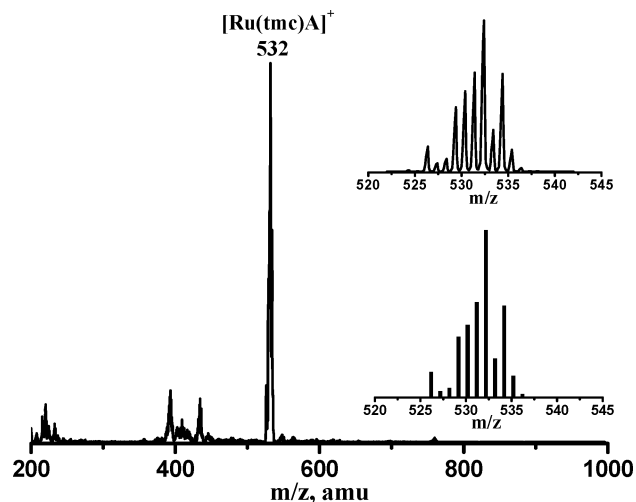
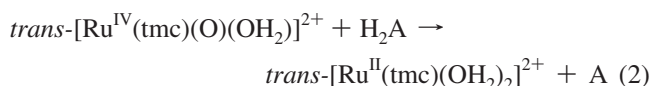
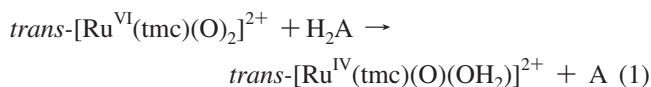
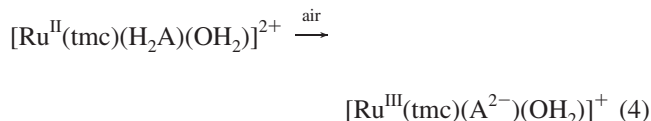
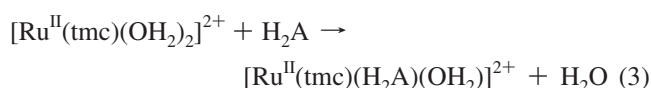


**Figure 3.** ESI mass spectrum of  $[\text{Ru}(\text{tmc})(\text{A})(\text{MeOH})](\text{BPh}_4)$  in the positive mode in acetone. The insets show the expanded isotopic distribution of the cluster at  $m/z = 532$  (upper) and the calculated isotopic patterns for  $[\text{Ru}(\text{tmc})(\text{A})]^+$  (lower).

first phase was observed; the ruthenium product was found to be *trans*- $[\text{Ru}^{\text{IV}}(\text{tmc})(\text{O})(\text{OH}_2)]^{2+}$  ( $\text{Ru}^{\text{IV}}$ ). On the other hand, when  $\text{Ru}^{\text{IV}}$  was reacted with 1 equiv or excess  $\text{H}_2\text{A}$ , the spectrophotometric changes were the same as that of the second phase. Analysis by  $^1\text{H}$  NMR indicated that 2 mol of dehydroascorbic acid (A) was produced from each mole of  $\text{Ru}^{\text{VI}}$ . Hence the two phases of the reaction correspond to  $\text{Ru}^{\text{VI}} \rightarrow \text{Ru}^{\text{IV}}$  and  $\text{Ru}^{\text{IV}} \rightarrow \text{Ru}^{\text{II}}$ , as represented by eqs 1 and 2.



On a longer time-scale and in the presence of excess ascorbic acid, further reaction appeared to occur, but the spectrophotometric changes were very small. However, if the solution was exposed to air at the end of the second phase, the solution slowly turned from pale yellow to green, and a peak at 868 nm was developed (Figure 2c). When the reaction was carried out on a larger scale, a green solid could be isolated upon addition of  $\text{NaBPh}_4$ . Analysis of the green solid (after washing with MeOH) is consistent with the formula  $[\text{Ru}^{\text{III}}(\text{tmc})(\text{A}^{2-})(\text{MeOH})](\text{BPh}_4)$ . The compound has a room temperature magnetic moment of  $\mu_{\text{eff}} = 1.85 \mu_{\text{B}}$ , consistent with its formulation as a ruthenium(III) complex with a doubly deprotonated ascorbate ( $\text{A}^{2-}$ ) ligand. The ESI/MS of the complex in Figure 3 shows a peak at 532  $m/z$  that is assigned to  $[\text{Ru}(\text{tmc})(\text{A})]^+$ . The reactions occurring after phase two may be represented by eqs 3 and 4.



**Kinetics.** In the presence of at least 10-fold excess of  $\text{H}_2\text{A}$ , clean pseudo-first-order kinetics were observed for over 3 half-lives for both phases. The pseudo-first-order rate constants,  $k_{\text{obs}}$ , are independent of  $[\text{Ru}^{\text{VI}}]$  ( $5 \times 10^{-5}$  to  $2 \times 10^{-4}$  M), but depend linearly on  $[\text{H}_2\text{A}]$  ( $1 \times 10^{-3}$  to  $2 \times 10^{-2}$  M) at 298.0 K and  $I = 0.1$  M. The second-order rate constants for the first ( $k_2$ ) and second ( $k_2'$ ) phases were found to be  $(2.58 \pm 0.04) \times 10^3 \text{ M}^{-1} \text{ s}^{-1}$  at pH = 1.19 and  $(1.90 \pm 0.03) \text{ M}^{-1} \text{ s}^{-1}$  at pH = 1.24, respectively. A few experiments were done by using  $\text{Ru}^{\text{IV}}$  as the oxidant, and the rate constants obtained were the same as that of the second phase (i.e.,  $k_2'$ ) of the reduction of  $\text{Ru}^{\text{VI}}$ .

**Effects of Acidity.** The effects of acidity on  $k_2$  were studied over the pH range 1.1–3.1 (Figure 4); at higher pH, the rates were too fast to be followed even by stopped-flow. The effects of pH on  $k_2'$  were studied over a wider pH range of 1.2–4.5. Both  $k_2$  and  $k_2'$  show a similar dependence on pH according to eqs 5 and 6.

$$k_2 = \frac{k_b}{[\text{H}^+]/K + 1} \quad (5)$$

$$k_2' = \frac{k_b'}{[\text{H}^+]/K + 1} \quad (6)$$

$K$  is the acid dissociation constant of  $\text{H}_2\text{A}$ . A nonlinear least-squares fit of the data gives  $k_b = (2.86 \pm 0.72) \times 10^6 \text{ M}^{-1} \text{ s}^{-1}$  and  $K = (9 \pm 2) \times 10^{-5} \text{ M}$  for the first phase,  $k_b' = (1.49 \pm 0.08) \times 10^3 \text{ M}^{-1} \text{ s}^{-1}$  and  $K = (6.0 \pm 0.6) \times 10^{-5} \text{ M}$  for the second phase. The values of  $K$  are in reasonable agreement with a literature value of  $1 \times 10^{-4} \text{ M}$ .<sup>8</sup>

**Kinetic Isotope Effects.** For the first phase of the reactions, the kinetics were investigated at two different pD values in  $\text{D}_2\text{O}$  at 298.0 K and  $I = 0.1$  M. The solvent

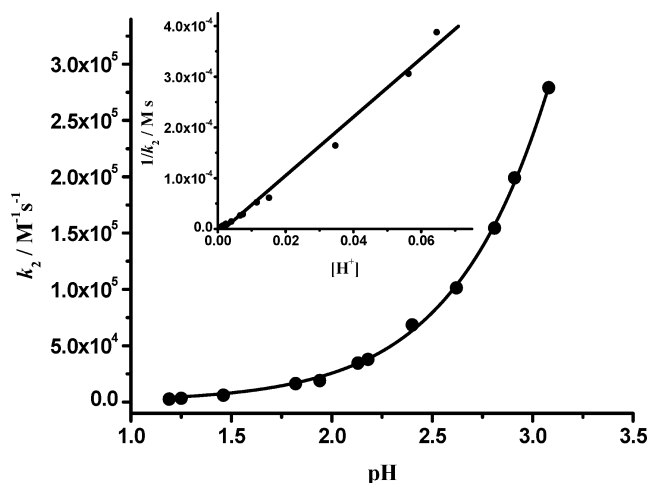


**Figure 4.** Plot of  $k_2$  vs pH for the first phase of the oxidation of  $\text{H}_2\text{A}$  by *trans*- $[\text{Ru}^{\text{VI}}(\text{tmc})(\text{O})_2]^{2+}$  at 298.0 K and  $I = 0.1$  M. The inset shows the corresponding plot of  $1/k_2$  vs  $[\text{H}^+]$  [slope =  $(5.77 \pm 0.19) \times 10^{-3}$ ; y-intercept =  $(-1.0 \pm 0.5) \times 10^{-5}$ ;  $r = 0.995$ ].

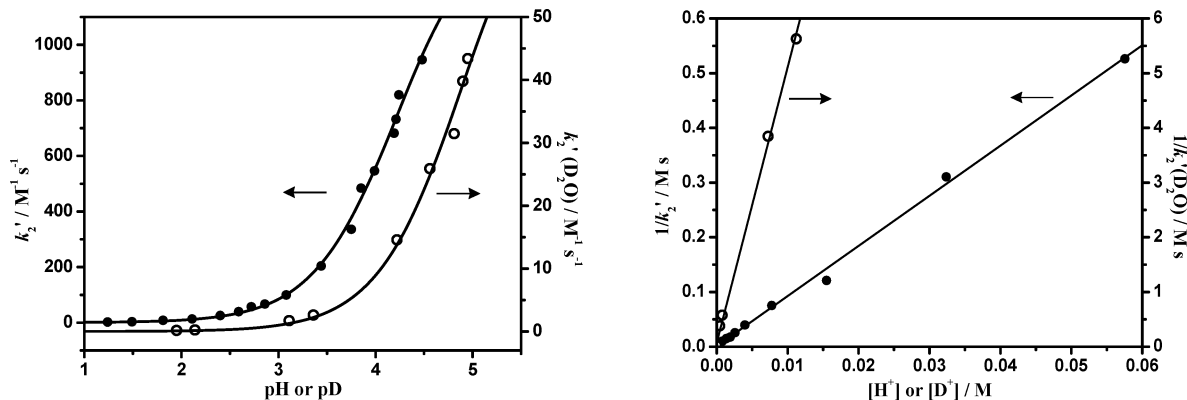


**Figure 5.** Left panel: Plot of  $k_2'$  vs pH (pD) for the second phase of the oxidation of  $\text{H}_2\text{A}$  by  $\text{trans-}[\text{Ru}^{\text{VI}}(\text{tmc})(\text{O})_2]^{2+}$  at 298.0 K and  $I = 0.1 \text{ M}$  in  $\text{H}_2\text{O}$  (●) and  $\text{D}_2\text{O}$  (○). Right panel: The corresponding plot of  $1/k_2'$  vs  $[\text{H}^+]$  ( $[\text{D}^+]$ ). For  $\text{H}_2\text{O}$ : slope =  $(9.17 \pm 0.11)$ ; y-intercept =  $(7.7 \pm 18.1) \times 10^{-4}$ ;  $r = 0.999$ . For  $\text{D}_2\text{O}$ : slope =  $(5.03 \pm 0.08) \times 10^2$ ; y-intercept =  $(7.2 \pm 3.5) \times 10^{-2}$ ;  $r = 0.999$ .

kinetic isotope effects are  $k_2(\text{H}_2\text{O})/k_2(\text{D}_2\text{O}) = (5.1 \pm 0.3)$  and  $(5.0 \pm 0.3)$  at  $\text{pH} = 1.95$  and  $2.77$ , respectively. For the second phase of the reactions, the kinetics were carried out in  $\text{D}_2\text{O}$  at  $\text{pD} = 1.95\text{--}4.95$ , and the plot of  $k_2'$  versus  $[\text{D}^+]$  is shown in Figure 5. A nonlinear least-squares fit of the data to eq 7 (Figure 5) gives  $k_b'(\text{D}_2\text{O}) = (7.71 \pm 1.10) \times 10^1 \text{ M}^{-1} \text{ s}^{-1}$  and  $K_D = (1.00 \pm 0.35) \times 10^{-5} \text{ M}$  at 298.0 K and  $I = 0.1 \text{ M}$ . A literature value for  $K_D$  is  $1.34 \times 10^{-5} \text{ M}$ .<sup>41</sup> The deuterium isotope effect is  $k_b'(\text{H}_2\text{O})/k_b'(\text{D}_2\text{O}) = (19.3 \pm 2.9)$ .

$$k_2'(\text{D}_2\text{O}) = \frac{k_b'(\text{D}_2\text{O})}{[\text{D}^+]/K_D + 1} \quad (7)$$

**Activation Parameters.** The effects of temperature on the oxidation of  $\text{H}_2\text{A}$  were studied from around 280 to 310 K at  $I = 0.1 \text{ M}$ . Activation parameters were obtained from the plot of  $\ln(k_2/T)$  versus  $1/T$  according to the Eyring equation. For oxidation by  $\text{Ru}^{\text{VI}}$ ,  $\Delta H^\ddagger$  and  $\Delta S^\ddagger$  were found to be  $(8.9 \pm 0.4) \text{ kcal mol}^{-1}$  and  $-(6 \pm 1) \text{ cal mol}^{-1} \text{ K}^{-1}$ , respectively, at  $\text{pH} = 2.71$ . For oxidation by  $\text{Ru}^{\text{IV}}$ ,  $\Delta H^\ddagger$  and  $\Delta S^\ddagger$  are found to be  $(9.5 \pm 0.5) \text{ kcal mol}^{-1}$  and  $-(16 \pm 2) \text{ cal mol}^{-1} \text{ K}^{-1}$ , respectively, at  $\text{pH} = 3.51$ .

**Computational Method.** The O–H bond dissociation energy (BDE) and the proton affinity (PA) of ascorbic acid and its conjugate bases in the gas phase have been calculated. The structures of ascorbic acid and its conjugate bases have been optimized at the B3LYP/6–311++G(2df,p) level.<sup>42</sup> On the basis of the optimized geometries, single-point energies were calculated at the MP2/6–311++G(2df,p) level. The harmonic vibration frequencies were also computed at the B3LYP/6–311++G(2df,p) level for the zero-point energy correction. It was found that the PAs and BDEs of the hydroxyl groups on the five-member-ring were significantly smaller than those of the side chain. Thus, only the PAs and BDEs for the hydroxyl groups on the ring are reported here. Figure 6 shows the energetic profile for the deprotonation and the O–H bond breaking processes in ascorbic acid. The PA for ascorbate is found

to be  $+311 \text{ kcal mol}^{-1}$ . The BDEs of  $\text{H}_2\text{A}$  and  $\text{HA}^-$  are calculated to be 83 and  $71 \text{ kcal mol}^{-1}$ , respectively. The lower BDE of  $\text{HA}^-$  than  $\text{H}_2\text{A}$  is probably due in part to stabilization of  $\text{A}^{\cdot-}$  by resonance.

## Discussion

The observed acid dependence of  $k_2$  and  $k_2'$  are consistent with  $\text{HA}^-$  being the kinetically active species (eqs 8–10).



Since the reduction potentials and the self-exchange rates of both  $[\text{Ru}^{\text{VI}}(\text{tmc})(\text{O})_2]^{2+}/[\text{Ru}^{\text{V}}(\text{tmc})(\text{O})_2]^+$  ( $E^0 = 0.56 \text{ V}$  vs NHE,  $k_{11} = 1 \times 10^5 \text{ M}^{-1} \text{ s}^{-1}$ )<sup>36</sup> and  $\text{HA}^{\cdot-}/\text{HA}^-$  ( $E^0 = 0.71 \text{ V}$ ,  $k_{22} = 1 \times 10^5 \text{ M}^{-1} \text{ s}^{-1}$ )<sup>11</sup> are known, the rate constant ( $k_{12}$ ) for the outer-sphere oxidation of  $\text{HA}^-$  by  $\text{Ru}^{\text{VI}}$  can be estimated using the Marcus cross-relation.<sup>43</sup>  $k_{12}$  is calculated to be  $4.6 \times 10^3 \text{ M}^{-1} \text{ s}^{-1}$  at 298.0 K (neglecting work terms), which is almost 3 orders of magnitude slower than the experimental rate constant ( $k_b = 2.86 \times 10^6 \text{ M}^{-1} \text{ s}^{-1}$ ); hence, an outer-sphere electron-transfer pathway may be neglected. On the other hand, the large deuterium isotope effect of 5.1 is consistent with an HAT mechanism. Similarly, in the oxidation of  $\text{HA}^-$  by  $\text{Ru}^{\text{IV}}$ , an electron transfer mechanism can be neglected since this will result in the formation of an unstable ruthenium(III) oxo species,  $[\text{Ru}^{\text{III}}(\text{tmc})(\text{O})(\text{OH}_2)]^+$ . Again, the large deuterium isotope effect of 19.3 is consistent with an HAT mechanism.

Mayer and co-workers have shown that the rates of a number of HAT reactions correlate with the bond dis-

(41) Yau, K. W. *Ph.D. Thesis*, City University of Hong Kong, 2003.

(42) Beck, A. D. *J. Chem. Phys.* **1993**, *98*, 5648–5652.

(43) Marcus, R. A.; Eyring, H. *Annu. Rev. Phys. Chem.* **1964**, *15*, 155–196.

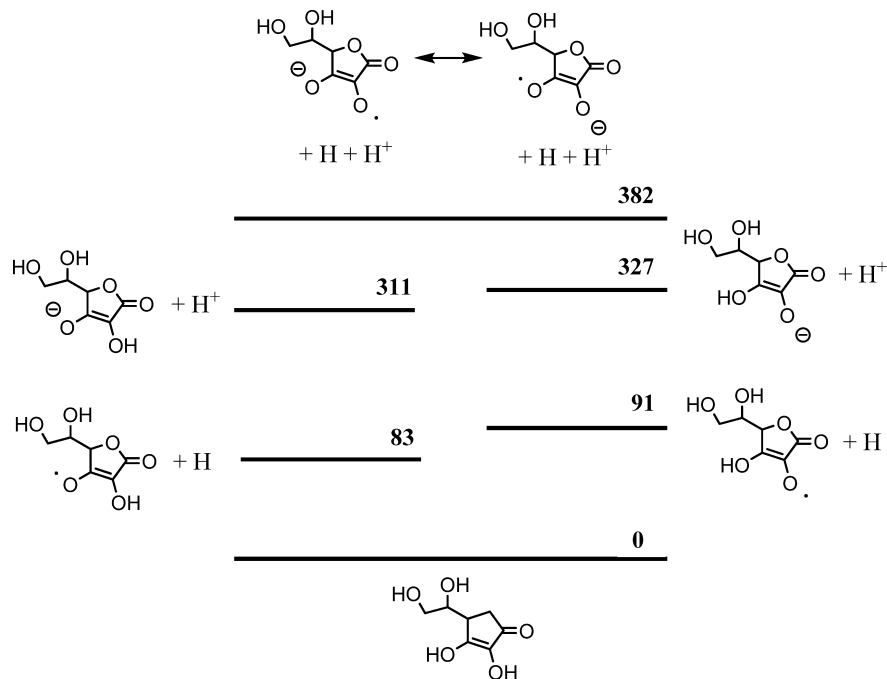


**Figure 6.** The energetic profile at 298 K for the deprotonation and the O–H bond breaking processes in ascorbic acid at the MP2/6–311++G(2df,p)//B3LYP/6–311++G(2df,p) level. All energies, in kcal/mol, are relative to ascorbic acid.

sociation energies (BDEs) of the substrates.<sup>44–46</sup> We have also reported similar correlations in the oxidation of hydrocarbons<sup>47</sup> and phenols<sup>48</sup> by *trans*-[Ru<sup>VI</sup>(N<sub>2</sub>O<sub>2</sub>)(O)<sub>2</sub>]<sup>2+</sup>, and in the oxidation of hydroquinones by *trans*-[Ru<sup>VI</sup>(tmc)(O)<sub>2</sub>]<sup>2+</sup>.<sup>49</sup> Since HAT from both the ascorbate anion (HA<sup>−</sup>) and hydroquinones involve O–H bond cleavage, we are interested to see if the data for the oxidation of HA<sup>−</sup> by Ru<sup>VI</sup> would also fit into the linear correlation between rate constants and BDEs for the oxidation of hydroquinones. In our previous correlation, the BDEs of hydroquinones used were those in the gas phase calculated according to the method of Wright and co-workers.<sup>50</sup> In order to be consistent we have calculated the O–H BDE of H<sub>2</sub>A and HA<sup>−</sup> in the gas phase, which are 83 and 71 kcal mol<sup>−1</sup>, respectively. The much higher BDE of H<sub>2</sub>A than HA<sup>−</sup> is consistent with our kinetic results which indicate that HA<sup>−</sup> is the only reactive species. As shown in Figure 7, an excellent linear correlation is obtained when log(rate constant) is plotted against the O–H BDEs of HA<sup>−</sup> and selected hydroquinones (H<sub>2</sub>Q–X) in the gas phase. Such a correlation supports an HAT mechanism for the oxidation of HA<sup>−</sup> by Ru<sup>VI</sup>.

A simplified plausible mechanism for the oxidation of HA<sup>−</sup> by *trans*-[Ru<sup>VI</sup>(tmc)(O)<sub>2</sub>]<sup>2+</sup> in aqueous solutions is summarized in eqs 11–15. Equations 12, 14, and 15

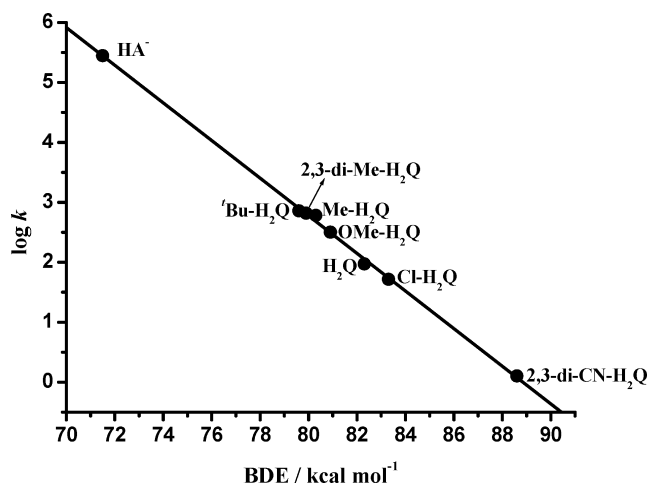
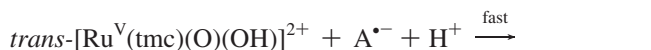
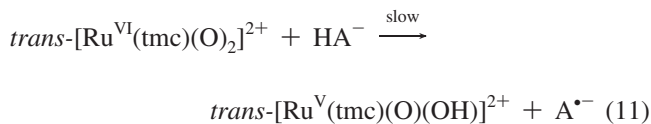
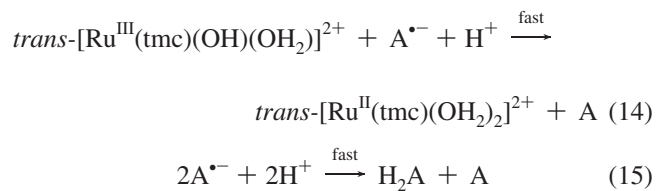


**Figure 7.** Plot of log *k* vs O–H BDEs for the oxidation of HA<sup>−</sup> and hydroquinones by *trans*-[Ru<sup>VI</sup>(tmc)(O)<sub>2</sub>]<sup>2+</sup> in aqueous solutions at 298.0 K and *I* = 0.1 M [slope =  $-(3.14 \pm 0.05) \times 10^{-1}$ ; y-intercept =  $(2.79 \pm 0.04) \times 10^1$ ; *r* =  $-0.999$ ].

represent the major reactions that occur after the slow steps.



- (44) Meyer, J. M. *Acc. Chem. Res.* **1998**, *31*, 441–450.  
 (45) Gardner, K. A.; Kuehnert, L. L.; Mayer, J. M. *Inorg. Chem.* **1997**, *36*, 2069–2078.  
 (46) Cook, G. K.; Mayer, J. M. *J. Am. Chem. Soc.* **1995**, *117*, 7139–7156.  
 (47) Lam, W. W. Y.; Yiu, S. M.; Yiu, D. T. Y.; Lau, T. C.; Yip, W. P.; Che, C. M. *Inorg. Chem.* **2003**, *42*, 8011–8018.  
 (48) Yiu, D. T. Y.; Lee, M. F. W.; Lam, W. W. Y.; Lau, T. C. *Inorg. Chem.* **2003**, *42*, 1225–1232.  
 (49) Lam, W. W. Y.; Lee, M. F. W.; Lau, T. C. *Inorg. Chem.* **2006**, *45*, 315–321.  
 (50) Wright, J. S.; Johnson, E. R.; DiLabio, G. A. *J. Am. Chem. Soc.* **2001**, *123*, 1173–1183.



HAT from  $\text{HA}^-$  to  $\text{Ru}^{\text{VI}}$  or  $\text{Ru}^{\text{IV}}$  would produce  $\text{A}^{\bullet-}$ , which is rapidly oxidized by  $[\text{Ru}^{\text{V}}(\text{tmc})(\text{O})(\text{OH})]^{2+}$  or  $[\text{Ru}^{\text{III}}(\text{tmc})(\text{OH})(\text{OH}_2)]^{2+}$  to give A.  $\text{A}^{\bullet-}$  may also undergo a rapid disproportionation reaction to give  $\text{H}_2\text{A}$  and A; the rate constant of this reaction at  $[\text{H}^+] = 0.1\text{--}1.0\text{ M}$  has been estimated to be  $\geq 10^8\text{ M}^{-1}\text{ s}^{-1}$ .<sup>51</sup> Further reaction

(51) Bielski, B. H. J.; Allen, A. O.; Schwarz, H. A. *J. Am. Chem. Soc.* **1981**, *103*, 3516–3518.

involving anation of  $[\text{Ru}^{\text{II}}(\text{tmc})(\text{OH}_2)_2]^{2+}$  by  $\text{H}_2\text{A}$  occurs, and the species  $[\text{Ru}^{\text{III}}(\text{tmc})(\text{A}^{2-})(\text{MeOH})]^+$  can be isolated upon aerial oxidation of the solution.

**Acknowledgment.** The work described in this paper was supported by the City University of Hong Kong (7001925).

**Supporting Information Available:** Additional tables and figures. This material is available free of charge via the Internet at <http://pubs.acs.org>.

IC8015904